J. Basic. Appl. Sci. Res., 6(7)15-23, 2016

ISSN 2090-4304
Journal of Basic and Applied Scientific Research
www.textroad.com

Automatic Cancerous Tissue Classification using Discrete Wavelet Transformation and Support Vector Machine

Usman Ali[1,*], Arslan Shaukat[2], Masroor Hussain[1], Jehad Ali[1], Khalil Khan[3], Muhammad Bilal Khan[1], Mumtaz Ali Shah[1]

[1]Faculty of Computer Science and Engineering, Ghulam Ishaq Khan Institute of Engineering Sciences and Technology, Topi, Pakistan
[2]Department of Computer Engineering, College of Electrical and Mechanical Engineering, National University of Science and Technology, Islamabad, Pakistan
[3]Department of Information Engineering, University of Brescia, Italy

Received: April 20, 2016
Accepted: June 29, 2016

ABSTRACT

Prostate cancer is one of the most common and dreadful type of cancer in men. The diagnosis of prostate cancer is difficult because of unclear symptoms and requires multiple procedures. A prostate tissue biopsy is used to detect the presence of cancer in the tissue. Pathologists assign a Gleason grade to the tissue, which determines the severity of the cancer. In a traditional examination, pathologists have to look at the tissue biopsy under microscope. Recently, with the development in digital pathology field, slides of glass tissues can be digitized for tissue images generation which is known as histological images (HI).These images are mostly used as a tool for diagnosis and classification of prostate cancer. Histological grading of these images is used to determine the level of malignancy or aggressiveness of cancerous tissues. Determining accurate grading is very important, because the pathologists use this information to help guide the treatment options for patients. Pathologists perform the grading manually so their experience directly influences the accuracy of grading. Therefore, for cancerous tissues grading an automatic technique will be required.

This research paper deals with design and development of Computer aided diagnosis (CAD) system for automatic grading of histological images of prostate cancer tissue. Our CAD system is based on 2D-Discrete Wavelet Packet Decomposition and Support Vector Machines (SVM). The algorithm is successfully applied to the classification of histological images of prostate cancer obtained from WebPathology, which provides high quality of histological images. We have obtained a classification accuracy of 92.24%.

KEYWORDS: Histological images, Gleason grading pattern, discrete wavelet packet decomposition, texture features

1. INTRODUCTION

Prostate cancer is the most common and dreadful type of cancer in men. Since there are no clear symptoms of prostate cancer so its diagnosis is difficult, and requires multiple procedures to detect the presence of disease. One of the most important step in detection of cancer in the tissue is the examination of the prostate tissue biopsy. If cancer is present in the tissue then second step is finding its Gleason grade which determines the severity of the cancer. In a traditional examination of cancer detection, pathologists have to look at the tissue biopsy under microscope. Now With the development in digital pathology field, slides of glass tissues can be digitized for tissue images generation which is known as histological images (HI). The key for controlling cancer is its early detection because cause of cancer still remains unknown; consequently early diagnosis can increase the treatment success rate. HI is a widely used tool for diagnosis and classification of prostate cancer.

Histological grading of these images is used to determine level of malignancy of cancerous tissues. Thus determining accurate grade of tissue is very important, because the pathologists use grade information for treatment options. Pathologists perform the grading process manually and their experience directly influences the accuracy of grading. Grading made by humans is not only time consuming and difficult but also subjective to observes; different grade may be assigned to same tumour by same pathologist when assessment is repeated [1]. Therefore automatic grading system is needed that can grade a sample tissue image automatically which will be beneficial for prostate cancer tissue images detection and classification.

***Corresponding Author:** Usman Ali, Faculty of Computer Science and Engineering, Ghulam Ishaq Khan Institute of Engineering Sciences and Technology, Topi, Pakistan.

Due to recent development in digital pathology, Digital image can be generated from glass tissue slides of biopsy samples. These images are called histological images and are used for analysis. The pathologist can determine the grade by viewing these histological images. Histological grade represents the aggressiveness level of cancer. Therefore assigning grade to these histological images is very important because this grade information is used in cancer prognosis and treatment planning. In digital pathology Researchers have been awared with the importance of quantitative assessment of histological images. This assessment can be utilized to support the decision of the pathologist about the existence of the cancer. Automatic grading of histological image of prostate cancer tissue can be divided into two main categories, namely cancer detection and classification i.e. assigning grade to these images [2]. However, most of the studies in the literature address the classification problem of histological images. In this problem, the aim is to classify a given sample of histological image of prostate cancer into one of the two classes, i.e. cancerous tissue and normal tissue, or into one of the multiple classes: normal, grade 3, 4 and 5 [3, 4]. The published studies in the literature have either used a segmentation-based approach i.e. Gland segmentation followed by gland feature extraction or used a segmentation-free approach, i.e. directly extracting texture features from the image itself. The motivation behind this research is to show a complete review of the modern CAD techniques used for automatic classification of histological images.

The rest of the paper is organized as follows: Section 2 gives an overview of the literature. Section 3 discusses image decomposition using discrete wavelet transform and discrete wavelet packet decomposition. Section 4 presents extraction of features for classification. Section 5 presents experimental results and finally a Section 6 presents summary and discussion.

2. LITERATURE REVIEW

Pathology is the study of cells and tissues of living organisms under microscope for disease detection. For cancer detection biopsy samples which are tissues taken from a human body are processed and its sections are placed onto a glass slider to observe them under microscope [5]. The microscopic analysis is used to identify morphological characteristics of tissues, which indicates the presence of cancer. Microscopic analysis of tissues is the only perfect method for verification of the existence of the cancer, and cancer grading which is the measurement of cancer severity. Due to recent development in digital pathology, digital image can be generated from glass tissue slides of biopsy samples. These images are called histological images and are used for analysis. The Pathologist can determine the grade by viewing these histological images. Histological grade represents the aggressiveness level of cancer. Therefore assigning grade to these histological images is very important because this grade information is used in cancer analysis and diagnoses planning. Histological grading is used to determine the severity of the cancer in the tissue. Pathologist uses Hematoxylin-Eosin (H&E) staining because Hematoxylin makes cell nuclei color blue and Eosin makes cytoplasm pink [6]. After staining, pathologists can decide the grade by observing the microscopic image of the tissue. The grading process can be done in two steps i.e. detection of cancer in the tissue, and assigning grade to the tissue image [2]. To detect cancer the tissue image is examined at different magnifications. By using the Gleason grading method described in [7, 8], the pathologist assigns a Gleason grade based on the pathological tissue pattern present in the tissue image. The Gleason grading method defines five Gleason grades (from 1 to 5) corresponding to five different Gleason patterns. Figure 1 shows Gleason grading system in which grade 1 is the least aggressive and grade 5 is the most aggressive level of cancer.

A low grade pattern i.e. grade 1 or grade 2 is very similar to the normal while high grade pattern i.e. grade 4 or grade 5 is very different from the normal pattern. The glands in grade 1 and grade 2 have a well defined structure. Studies in the literature have recommended that Gleason grade 1 and 2 should rarely be used due to their uncommonness in the tissue [10, 11]. The pattern of grade 3 usually has small glands forming individual units and stay separated from each other and is the most common pattern. Glands in grade 4, tends to fuse with nearby glands so that gland structures become ill-defined. As a result, individual gland units are not easy to identify in this pattern. Finally grade 5 pattern is characterized by the total loss of gland structures, so that only sheets of cells are visible in this tissue pattern.

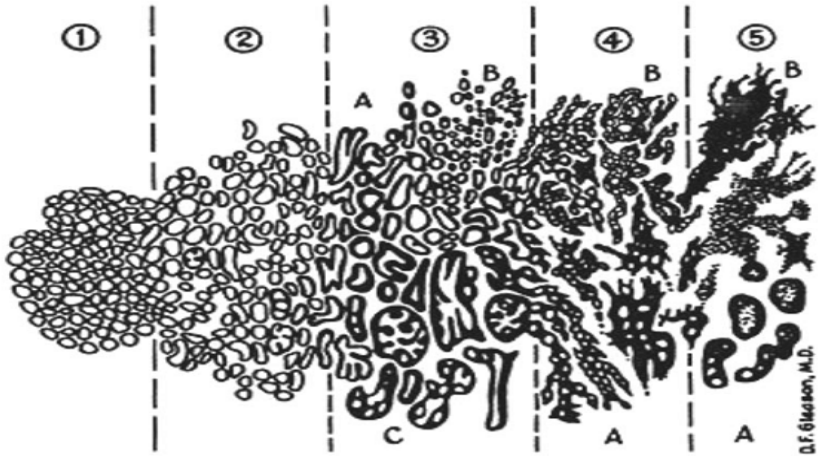

Figure 1. Gleason grading diagram [9]

The study of histological images has been an active area of research since last few years [12–14]. The beginning of this research started in early 90s [15] but relatively in low number, apparently due to the less saturation of the digital apparatus in pathology. Contemporary improvements in digital pathology, various cancer grading methods have been suggested, including brain [16], breast [17], cervix [18], liver [19], lung [20] and prostate [21, 22] cancer grading. Analyses on the automated grading dependent on histological images are already present in the previous studies [23-25], dealing with various kinds of problems related with multiple image modalities

Stotzkaetal. [12] proposed a method to discriminate between poorly and moderately differentiated prostate tissues. Their results are based on the immense number of texture features and shape of the tissue image. On the basis of these features they used neural network to classify tissue images. Wetzel et al. [13] suggested content-based tissue image retrieval for Gleason grading of prostate tissues. Their results do not directly attempt to reproduce the pathologist's view. Rather, it depends on comparison of tissue image features with similar features of previously graded tissue image from database. Smithet al. [14] suggested a measurement technique for Gleason grading of tissue histological images, which is based on Eigen values and Fourier transform. Their method is able to differentiate 35 images grades out of 36 images data set. The limitation of their method is that it could not distinguish between grades 4 and 5.

3. Image Decomposition

Since Gleason grading of prostate cancer is based on architecture of the glands, not shape information of individual cells [9]. It means that grading of HI primarily depend on texture properties of the image. Wavelet transformation is the most suitable tool used for texture analysis of image [26-29] for classification. Therefore wavelet transformation can be used to extract texture feature of the given image. Wavelet transformation is used to decompose a given image into series of sub-band images. Texture features is extracted from these sub-band images. Discrete Wavelet Transform (DWT) is used to divide the input image into sub bands known as Approximation sub band (LL), Vertical sub band (LH), Horizontal sub band (HL), and Diagonal sub band (HH) at each level. Figure 2 shows level 1 decomposition of input image. In next level only approximation sub band is further decomposed into four new sub bands (approximation, horizontal, vertical, diagonal) these new sub bands are represented by LLLL, LLHL, LLLH and LLHH respectively.

In the literature most of the wavelet based techniques [26-28] as discussed earlier, uses pyramidal decomposition in which sub bands of low frequency is decomposed repeatedly to form new sub bands until a predefined level is reached.

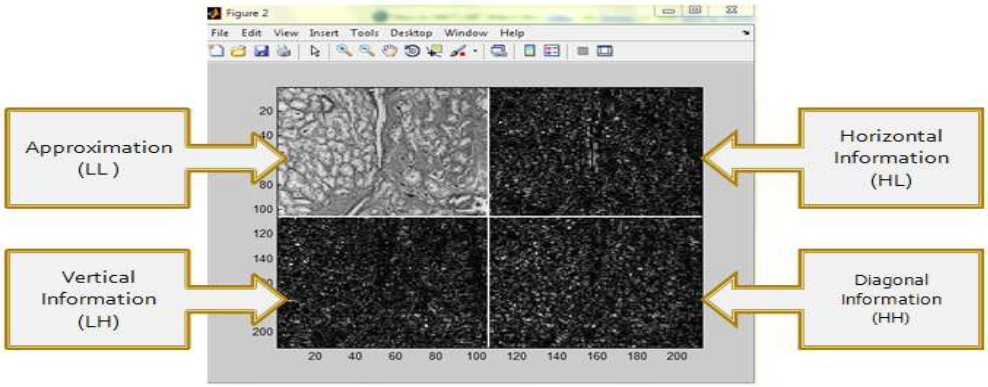

Figure 2. Level 1 decomposition showing 4 sub bands

However the limitation of using such method is that, it does not take benefit of the features of high frequency sub bands. As we know that image texture features are mostly focused in high frequency bands [30]. In order to overcome this limitation discrete wavelet packet decomposition is developed which decomposes the high frequency sub bands as well [31] and provides complete representation of image for classification using texture properties of the image.

3.1. Discrete Wavelet Packet Decomposition (DWPD)

Discrete Wavelet Packet Decomposition (DWPD) is an extension of DWT in which the only approximation sub-band is further decomposed. While in discrete wavelet packet decomposition all the four sub bands are decomposed further. In DWT low frequency are grouped into narrow bands as only the approximation sub band is repeatedly decomposed, which contains the lowest frequency, While DWPD also decomposes the high frequency bands at the cost of increased computational complexity. DWPD computes all possible sub bands of the image at a particular level. All of these sub bands do not carry equal information, some sub bands carry less information and some sub bands carry most or optimal information which are sufficient for image representation. Our proposed algorithm is based on DWPD which devides the image into all sub bands by providing pre-defined number of level. Figure 3 shows 3 level DWPD of prostate tissue image.

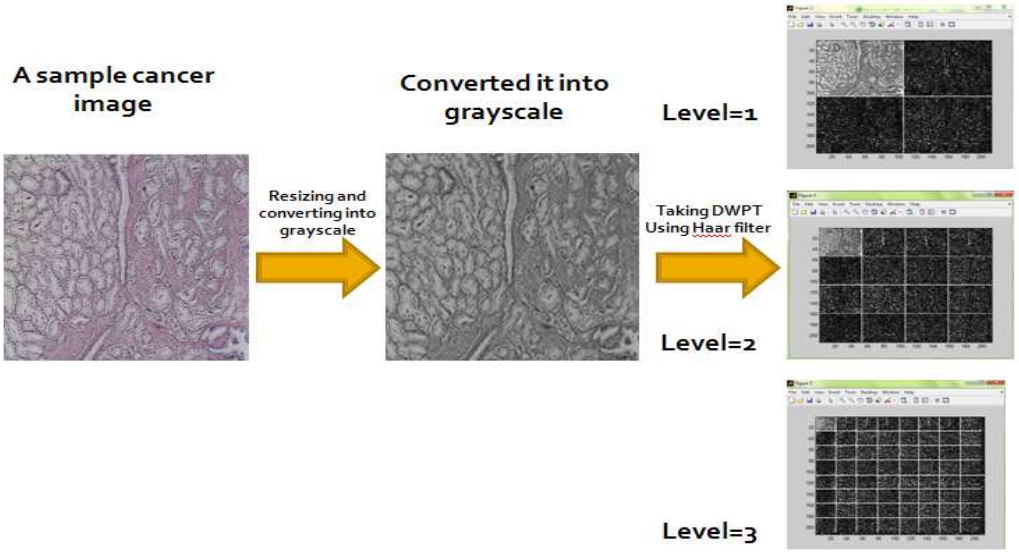

Figure 3. A 3 level DWPD showing all possible sub bands of an input image

An input tissue image is decomposed into 4 sub images in level 1. In level 2 each sub image of level 1 is further decomposed into 4 sub images which produce 16 (4 × 4) sub images. In level 3 each sub image of level 2 is further decomposed into 4 sub images which produce 64 (16 × 4) sub images and so on. Thus 3 level decomposition produce total 84 (4+16+64) sub images of a given input image.

4. Feature Extraction and Classification

4.1. Statistical Features

Statistical features based on Gray level Co-occurrence Matrix (GLCM), proposed by Haralick [32] are extracted from each sub band of the prostate tissue image. GLCM stores information that shows the frequency of a pixel with value *i* appears in a particular direction with a pixel with value *j*. Therefore GLCM is a matrix of co-occurring values at a given direction/offset. GLCMs are computed to perform spatial analysis of the sub-bands, which enable us to capture the spectral and texture properties of the image. In order to achieve a degree of rotation invariance GLCMs are computed for each sub-band in four directions i.e. 0^{θ}, 45^{θ}, 90^{θ} and 135^{θ} with a distance set from 1 to 4. Thus 16 GLCMs are computed for each sub-band. Each GLCM is normalized to 1 so that the sum of all the elements in GLCM is equal to 1. In the normalized GLCM each element (*i*, *j*) is the joint probability occurrence of pixel pair with a defined offset having values *i* and *j*. The normalization of each GLCM is done for extraction of following four statistical features.

i. **Correlation**: Correlation (Cr) is shown in below equation. It shows how coefficients of sub bands correlated with its neighbor over the entire sub band.

$$Cr = \sum_{i,j} \frac{(i-\mu i)(j-\mu j)\,p(i,j)}{\sigma_i \sigma_j} \quad (1)$$

where, μ, σ and $p(i, j)$ represents mean, variance and joint probability of sub image respectively. The value of correlation is 1 for perfectively positive sub band and -1 for negatively sub band. Correlation is not defined for constant sub band.

ii. **Contrast**: Contrast (Ct) is the difference between coefficients values over a sub band and is shown in below equation:

$$Ct = \sum_{i,j} (|i-j|^2\, p(i,j) \quad (2)$$

***Note: -** Contrast value will be zero for a constant sub-band.

iii. **Energy:** It is the most important feature which describe whether a texture is present or not in a given sub band. The following equation is used to calculate the energy (E) of a given sub band:

$$E = \sum_{i,j} p(i,j)^2 \quad (3)$$

iv. **Homogeneity:** It is the opposite of contrast and is a measure of the closeness of the distribution of elements in GLCM to the GLCM diagonal, as the diagonal elements represent pixel pairs with no difference in values. Homogeneity (H) can be calculated in below equation:

$$H = \sum_{i,j} \frac{p(i,j)}{1+|i-j|} \quad (4)$$

For each sub image we extract 4 statistical features (contrast, correlation, energy and homogeneity). We have total 84 sub images for a single input image. Thus for a single input image we have 336 (84 × 4) features.

4.2. Classification using Support Vector Machines

After extraction of statistical features, prostate cancer tissue images are classified on the bases of these features. We used binary SVM classifier for classification task. We used multiclass SVM implementation provided by Neuburger [33]. LIBSVM default kernel function, which is a Radial Basis function (RBF), is used for training. Figure 4 represents flowchart of the overall framework.

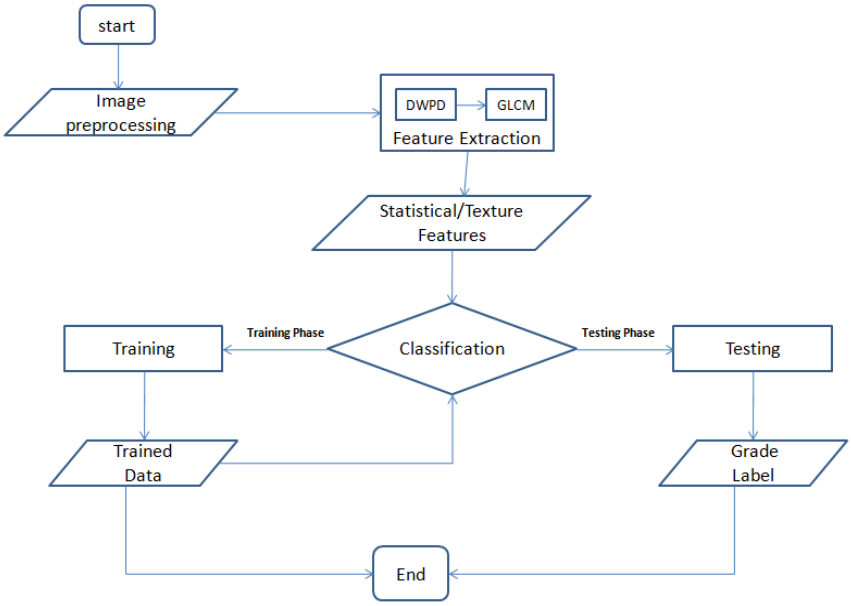

Figure 4. Flow chart of proposed cancerous tissue classification algorithm

5. Experimental Results

The efficiency of the proposed technique for cancerous tissue classification is tested using the images from Webpathology [34, 35]. The images are in color and of different size. These images were preprocessed i.e. resized into the same size of 500 × 324 pixels and converted into gray scale as color of image does not carry useful information in Gleason grading process. We finally obtained 43 images of grade 3, 44 images of grade 4 and 42 images of grade 5. We excluded grade 1 and grade 2 in our classification because they are very rare and also they are very similar to normal tissues. We used Haar Wavelet filter for wavelet decomposition up to level 3 for calculating sub images of the given input image. Several experiments were conducted to analyze the behavior of results with respect to changes in training and testing images dataset. We used 10-fold cross-validation protocol in which the training set is divided into 10 subsets -- 9 subsets are used for training and remaining one is used for testing. Table 1 shows experimental results.

Table 1 shows the average classification accuracy for grade 3, grade 4 and grade 5 in each experiment. The purpose of these experiments are to explore the efficiency of the proposed algorithm with changing in training and testing images dataset and also to find out the optimum number of tissue images dataset that can be used for training and template creation to achieve better results. Table 2 shows individual average accuracies for grade 3, grade 4 and grade 5.

Table 1. Experimental results

Exp. No	Training images	Test images	Correctly classified	Classification rate %
1	117	12	11	91.66
2	116	13	11	84.61
3	116	13	13	100.00
4	116	13	13	100.00
5	116	13	12	92.30
6	116	13	11	84.61
7	116	13	11	84.61
8	116	13	11	84.61
9	116	13	13	100
10	116	13	13	100
Mean Accuracy				92.24
Standard Deviation				7.25

In the table 2 we observe that 119 out of 129 images were correctly classified which gives 92.24% overall average classification accuracy.

Table 2. Average Classification Rate for Each grade

Grade	Total Test images	Correctly Classified	Classification rate %
Grade 3	43	41	95.34
Grade 4	44	40	90.90
Grade 5	42	38	90.47
Total	129	119	92.24

5.1. Evaluation of our Classification Techniques

The accuracy of prostate cancer tissue image classification cannot be compared directly because there is no standard benchmark dataset of histological images of prostate cancer tissue available [36]. Each and every researcher acquired a unique dataset [2] from the specific hospital dealing with digital pathology, just because of the lack of a standard dataset. Section 5, First Paragraph gives a detail description of the dataset we used for our experiments. In order to provide relative measure of the performance of the classification technique and to facilitate such comparison, well known and widely accepted standard benchmark database of prostate cancer tissue image is needed. Table 3 shows our approach provides better results as compared to the existing techniques.

Table 3: Results comparison

References	Dataset	Segmentation	Classification	Accuracies
Gorelicketal. [37]	991 Prostate sub images	super-pixel image partitioning	AdaBoost	90% and 85%
Nguyen et al. [21]	17 H&E prostate WSI	Maximum object likelihood binarization	Intensity, morphology & texture with SVM	90 %
Ali et al. [22]	80 H&E Prostate WSI	Watershed, Shape prior based ACM in level set formation	Morphology with SVM	86 %
Usman et al.	129 H&E Prostate WSI	Segmentation free approach	DWPD , SVM	92.24%

The above table clearly shows that our classification accuracy of 92.24% is better than state-of-the-art work by Gorelicket al. [37], Nguyen et al. [21] and Ali et al. [22].

6. Conclusion

In this research work we have studied prostate cancer tissue histological image classification algorithm based on wavelet packet decomposition. The most important need for image classification techniques is that the extracted features of an image should be discriminative and uncorrelated. By using this principle, the features will generate very informative and compact representation of the image for classification purpose.

DWPD enable the decomposition of an image into various frequency sub-bands. This property enables it appropriate for the purpose of classification of texture images. Suitable features required to be extracted for texture image classification to make a representation which is more discriminative in the transform domain. Commonly used wavelet features are contrast, correlation, homogeneity and energy of each wavelet sub band. The over-complete structure of the wavelet packet decomposition motivates the selection of the wavelet features for classification.

REFERENCES

[1] Ojansivu, V., Linder, N., Rahtu, E., Pietikainen, M., Lundin, M., Joensuu, H., & Lundin, J., 2013. Automated classification of breast cancer morphology in histopathological images. Diagnostic Pathology, 8(1), 1-4.

[2] Nguyen, Kien., 2013. Contributions to computer-aided diagnosis of prostate cancer in histopathology, PhD Dissertation Michigan State University.

[3] Khurd, P., Bahlmann, C., Maday, P., Kamen, A., Gibbs-Strauss, S., Genega, E. M., & Frangioni, J. V. , 2010. Computer-aided Gleason grading of prostate cancer histopathological images using texton forests. In Biomedical Imaging: From Nano to Macro IEEE International Symposium, pp: 636-639.

[4] Khurd, P., Grady, L., Kamen, A., Gibbs-Strauss, S., Genega, E. M., & Frangioni, J. V., 2011. Network cycle features: Application to computer-aided gleason grading of prostate cancer histopathological images. In Biomedical Imaging: From Nano to Macro, 2011 IEEE International Symposium, pp: 1632-1636.

[5] Belsare, A. D., & Mushrif, M. M., 2012. Histopathological image analysis using image processing techniques: An overview. Signal & Image Processing, 3(4), 23.

[6] Gurcan, M. N., Boucheron, L. E., Can, A., Madabhushi, A., Rajpoot, N. M., & Yener, B., 2009. Histopathological image analysis: a review. Biomedical Engineering, IEEE Reviews in, 2, pp: 147-171.

[7] Gleason, D. F. , 1977. Histologic grading and clinical staging of prostatic carcinoma. Urologic pathology: the prostate, pp: 171-197.

[8] Gleason, Donald F. ,1992. Grading of prostate cancer: a perspective., Human pathology 23.3, pp: 273-279.

[9] Jafari-Khouzani, Kourosh, and Hamid Soltanian-Zadeh, 2003. Multiwavelet grading of pathological images of prostate., Biomedical Engineering, IEEE Transactions on 50.6, pp: 697-704.

[10] Epstein, Jonathan I, 2010. An update of the Gleason grading system., The Journal of urology 183.2, pp: 433-440.

[11] Iczkowski, Kenneth A., and M. Scott Lucia., 2011. Current perspectives on Gleason grading of prostate cancer., Current urology reports 12.3, pp: 216-222.

[12] Stotzka, R., Männer, R., Bartels, P. H., & Thompson, D., 1995. A hybrid neural and statistical classifier system for histopathologic grading of prostatic lesions. Analytical and quantitative cytology and histology/the International Academy of Cytology [and] American Society of Cytology, 17(3), pp: 204-218.

[13] Wetzel, A. W., Crowley, R., Kim, S., Dawson, R., Zheng, L., Joo, Y. M., ... & Becich, M. J., 1999. Evaluation of prostate tumor grades by content-based image retrieval. In The 27th AIPR Workshop: Advances in Computer-Assisted Recognition, International Society for Optics and Photonics, pp: 244-252.

[14] Smith, Y., Zajicek, G., Werman, M., Pizov, G., & Sherman, Y., 1999. Similarity measurement method for the classification of architecturally differentiated images. Computers and Biomedical Research, 32(1), 1-12.

[15] Bartels, P. H., Thompson, D., Bibbo, M., & Weber, J. E., 1992. Bayesian belief networks in quantitative histopathology. Analytical and quantitative cytology and histology/the International Academy of Cytology [and] American Society of Cytology, 14(6), pp: 459-473.

[16] Gurcan, M. N., Pan, T., Shimada, H., & Saltz, J., 2006. Image analysis for neuroblastoma classification: segmentation of cell nuclei. In Engineering in Medicine and Biology Society, EMBS'06. 28th Annual International Conference of the IEEE pp: 4844-4847.

[17] Street, W. Nick, William H. Wolberg, and Olvi L. Mangasarian., 1993. Feature extraction for breast tumor diagnosis, IS&T/SPIE's Symposium on Electronic Imaging: Science and Technology. International Society for Optics and Photonics.

[18] Keenan, S. J., Diamond, J., Glenn McCluggage, W., Bharucha, H., Thompson, D., Bartels, P. H., & Hamilton, P. W., 2000. An automated machine vision system for the histological grading of cervical intraepithelial neoplasia (CIN). The Journal of pathology, 192(3), 351-362.

[19] Huang, Po-Whei, and Yan-Hao Lai., 2010. Effective segmentation and classification for HCC biopsy images. Pattern Recognition 43.4, pp: 1550-1563.

[20] Di Cataldo, Santa, et al., 2010. Automated segmentation of tissue images for computerized IHC analysis., Computer methods and programs in biomedicine 100.1: 1-15.

[21] Nguyen, K., Jain, A. K., & Sabata, B., 2011. Prostate cancer detection: Fusion of cytological and textural features. Journal of pathology informatics, 2(2), 3.

[22] Ali, Sahirzeeshan, et al., 2011. Adaptive energy selective active contour with shape priors for nuclear segmentation and gleason grading of prostate cancer. Medical Image Computing and Computer-Assisted Intervention–MICCAI, pp: 661-669.

[23] Demir, Cigdem, and Bülent Yener., 2005. Automated cancer diagnosis based on histopathological images: a systematic survey., Rensselaer Polytechnic Institute, Tech. Report.

[24] He, L., Long, L. R., Antani, S., & Thoma, G., 2010. Computer assisted diagnosis in histopathology. Sequence and genome analysis: methods and applications, pp: 271-287.

[25] Gurcan, M. N., Boucheron, L. E., Can, A., Madabhushi, A., Rajpoot, N. M., & Yener, B., 2009. Histopathological image analysis: a review. Biomedical Engineering, IEEE Reviews in, 2, pp: 147-171.

[26] Liu, J. F., & Lee, J. C. M., 1996. An efficient and effective texture classification approach using a new notion in wavelet theory. In Pattern Recognition, Proceedings of the 13th International Conference, Vol. 2, pp: 820-824.

[27] Smith, J. R., & Chang, S. F., 1994. Transform features for texture classification and discrimination in large image databases. In Image Processing Proceedings ICIP-94., Vol. 3, pp: 407-411.

[28] Kokare, Manesh, Prabir K. Biswas, and Biswanath N. Chatterji., 2007. Texture image retrieval using rotated wavelet filters, Pattern recognition letters 28.10, pp: 1240-1249.

[29] Ojala, T. & Pietikainan, M., 2004. Texture Classification, Machine Vision and Media Processing Unit, University of Oulu, Finland.

[30] Taeprasartsit, Pinyo, and Liang Guo., 2004. Texture Analysis and Classification with Tree-Structured Wavelet Transform, May 2: 1-24.

[31] Coifman, R. R., and Y. Meyer., 1990. Orthonormal wave packet bases, preprint.

[32] Haralick, Robert M., 1979. Statistical and structural approaches to texture, Proceedings of the IEEE 67.5, pp: 786-804.

[33] Multiclass SVM implementation by Cody Neuburger cneuburg@fau.edu, Florida Atlantic University, Florida USA

[34] http://www.webpathology.com/image.asp?n=28&Case=20

[35] http://www.pathologyoutlines.com/topic/prostateGrading.html

[36] Irshad, H., Veillard, A., Roux, L., & Racoceanu, D., 2014. Methods for Nuclei Detection, Segmentation, and Classification in Digital Histopathology: A Review—Current Status and Future Potential. Biomedical Engineering, IEEE Reviews in, 7, pp: 97-114.

[37] Gorelick, Lena, et al., 2013. Prostate histopathology: Learning tissue component histograms for cancer detection and classification., Medical Imaging, IEEE Transactions on 32.10, pp: 1804-1818.